Edward D. Young, Ph.D.
University of California, Los Angeles

Science Progress for ACS PRF# 54848-ND2
"Process vs. Source for Methane Gas"

We have now achieved the goals of this project as illustrated in this summary document. The PRF grant was instrumental in attaining these goals.

In Figure 1 we show ~ 170 natural CH_4 samples analyzed and vetted in our laboratory at UCLA to date as well as microbe culture experiments and several high-temperature FTT experiments in $\Delta^{12}CH_2D_2$ vs. $\Delta^{13}CH_3D$ space on the left and in the traditional Schoell plot (δD vs. $\delta^{13}C$) on the right. Based on the clumping diagram, three groups of samples are selected as examples of "process endmembers" as a sort of test of the efficacy of considering process as a means of deducing provenance. Two of the three groups are easily defined and substantiated by laboratory experiments. The first of these are the natural samples that represent purely microbial methanogenesis based on their similarity to the combination of $\Delta^{12}CH_2D_2$ and $\Delta^{13}CH_3D$ values obtained in our *in-vitro* culture experiments (in most cases these are from boreal wetlands). The second group comprises gases produced at high temperatures (meaning > 100 ^oC) that lie at or near to isotopologue thermodynamic equilibrium. While many of these gases are thermogenic, we are purposefully avoiding the traditional classification terminology at this stage because these terms can connote both process and the sources of carbon and hydrogen (e.g., Sherwood Lollar et al. 2006; Etiope and Sherwood Lollar 2013). The third group represents "abiotic" methane. Here we have immediately deviated from the strategy outlined in the previous sentence and introduced a measure of circularity into the classification by convolving it with source material. This is justified because of the overwhelming geological and geochemical evidence suggesting that the Kidd Creek mine gases owe their origin to abiotic processes deep in the crust.

The three endmember processes are well separated on the left-hand panel of the Figure 1. Those same data points, with the same color coding, are plotted on the classical "Schoell plot" on the right in the Figure. I have added two major methane source fields, biotic and abiotic, as inspired by the fields shown in Etiope and Schoell (2014) and Etiope (2017). The microbial and thermogenic process subfields of the biotic field are also shown. Overall, the microbial gases as defined by the isotopic bond ordering plot in the microbial subfield for biotic gases in the Schoell plot. The high-T equilibrium gases tend to plot in the thermogenic subfield of the biotic field in the Schoell plot, and the Kidd Creek abiotic gases are at the lower edges of the abiotic field in the Schoell plot. Have we learned anything?

However, critically, we note that our new isotopologue fields separate process from source material unambiguously. For example, the vertical (δD) positions of boreal wetland microbial methanogenesis data in the Schoell plot are lower than those for many "typical" microbial gases because the water δD values for these arctic environs are ~ −200 ‰ (e.g., Douglas et al. 2016 and references therein), rather lower than for waters from lower latitudes. Our kinetic models predict a downward shift in δD of ~160 ‰ relative to the source hydrogen, yielding bulk dD values of about −360 ‰, consistent with the boreal wetland data in the Figure. The breadth of the microbial field in the Schoell plot is therefore dictated in part by the range of source hydrogen and carbon samples independent of process. In isotopic bond ordering space, this effect is normalized out.

The importance of normalizing away reactant bulk isotopic compositions is best exemplified by the fact that there are instances where data falling squarely in the microbial field in $\Delta^{13}CH_3D$ – $\Delta^{12}CH_2D_2$ space are not in the Biotic field on the Schoell plot. A glaring example is the highest $\delta^{13}C$ point from the Oman ophiolite that is evidently microbial in origin despite it's abiotic bulk isotope characteristics in the Schoell plot (Figure 1). The reasons can be traced to unexpected source materials (as enumerated in publications in preparation). Similarly, gases equilibrated at relatively high temperatures as evidenced in the $\Delta^{13}CH_3D$ – $\Delta^{12}CH_2D_2$ plot span the biotic and abiotic fields in the Schoell plot.

Most of the other data points that appear in the attached Figure (undifferentiated data are shown in grey) that do not fall within one of the fields in $\Delta^{13}CH_3D$ – $\Delta^{12}CH_2D_2$ space are the result of mixing, fractionation by molecular mass (e.g., Giunta et al. 2018), or possibly processes that are still under study (see next section).

References Cited

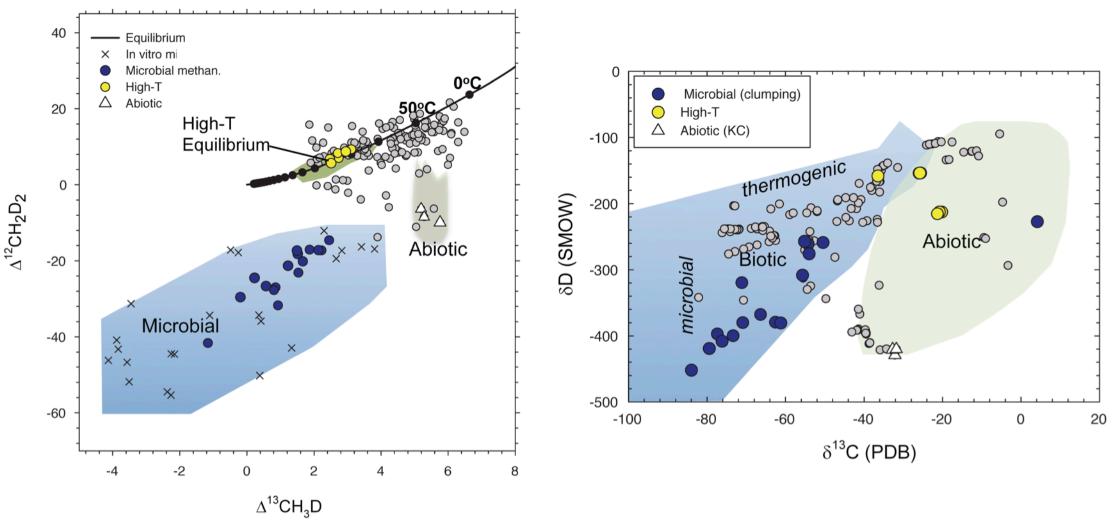

Figure 1. Comparison of data categorized by process in $\Delta^{12}CH_2D_2$ vs. $\Delta^{13}CH_3D$ space (left panel) to their positions in the bulk isotope "Schoell" plot (right panel). Details are discussed in the text. Fields on the left are from the mass-18 isotopologue work while the fields in bulk isotope space are from Etiope and Schoell (2014) and Etiope (2017). Grey symbols are data not categorized explicitly in this plot. The data labeled "Microbial methan." are dominantly, although not entirely, from Boreal lakes.

Douglas P. M. J., Stolper D. A., Smith D. A., Anthony K. M. W., Paull C. K., Dallimore S., Wik M., Crill P. M., Winterdahl M., Eiler J. M. and Sessions A. L. (2016) Diverse origins of Arctic and subarctic methane point source emissions identified with multiply-substituted isotopolouges. *Geochemica et Cosmochimica Acta* **188**: 163-188

Etiope G. (2017) Methane origin in the Samail ophiolite: Comment on "Modern water/rock reactions in Oman hyperalkaline peridotite aquifers and implications for microbial habitability" [Geochem. Cosmochim. Acta 179 (2016) 217-24]. *Geochemica et Cosmochimica Acta* **197**: 467-470

Etiope G. and Schoell M. (2014) Abiotic gas: atypical, but not rare. *Elements* **10**: 291-296

Etiope G. and Sherwood Lollar B. (2013) Abiotic Methane on Earth. *Reviews of Geophysics* **51**: 276-299

Giunta T., Young E. D., Warr O., Kohl I., Ash J. L., Martini A. M., Mundle S. A. C., Rumble D., Perez-Rodriquez I., Wasley M., LaRowe D. E., Gilbert A. and Sherwood Lollar B. (2018)

Methane sources and sinks in continental sedimentary basins: New insights from paired clumped isotopologues $^{13}CH_3D$ and $^{12}CH_2D_2$. *Geochemica et Cosmochimica Acta*: (in press)
McCollom T. M. (2016) Abiotic methane formation during experimental serpentinization of olivine. *Proceedings of the National Academy of Sciences* **113**: 13965-13970
Sherwood Lollar B., Lacrampe-Couloume G., Slater G. F., Ward J., Moser D. P., Gihring T. M., Lin L.-H. and Onstott T. C. (2006) Unravelling abiogenic and biogenic sources of methane in the Earth's deep subsurface. *Chemical Geology* **226**: 328-339